

## Fracture Behavior of Alumina Reinforced Magnesium-Alloy Nano Composites

Mr. S.Yesanna<sup>1</sup>, Mr. Renigunta Rajender<sup>2</sup>, Mr. G. Panindra Kumar<sup>3</sup>

<sup>1</sup>Professor, Department Of Mechanical, Faculty Of HITS, Hyderabad, India.

<sup>2</sup>Professor, Department Of Mechanical, Faculty Of HITS, Hyderabad, India.

<sup>3</sup>Asso. Professor, Department Of Mechanical, Faculty Of HITS, Hyderabad India.

**Abstract:** Fracture behaviour of nano alumina reinforced magnesium-alloy composites was investigated in terms of the plane strain fracture toughness (K<sub>IC</sub> or K<sub>IQ</sub>) and fracture mode. Also evaluated and reported are the corresponding Micro Hardness and Flexural Strength. The main aim of this paper was to determine the amount of Al<sub>2</sub>O<sub>3</sub> reinforcement that results into best combination of Flexural Strength and Micro Hardness. Magnesium nano composites containing 3.5, 7.0 and 14.0 volume percentage of Al<sub>2</sub>O<sub>3</sub>. Conditional fracture toughness (K<sub>IQ</sub>) is found to decrease moderately with increase in the crack length due to the change in fracture mode from grossly tensile to predominant shear which is further confirmed by the fractography. A consistently increasing R curve behaviour was indicated in both the materials with significant increase in total fracture energy release rate (J<sub>IC</sub>) with the normalised displacement ( $\delta/\delta_c$ ). Fractographic analysis followed by property index calculations clearly shows that property index remains almost constant with respect to the property for the two process conditions and thus, confirming the fact that the extent of quasi cleavage facet controls the fracture shown. A higher value of property indices again indicates that the 7 Vol.% Al<sub>2</sub>O<sub>3</sub> material exhibits better strength properties, which was found to result in increase in fracture resistance bringing out the fact the 3.5 Vol.% Al<sub>2</sub>O<sub>3</sub> materials, studied here obey SEM.

**Keywords:** Al<sub>2</sub>O<sub>3</sub>, SEM, XRD, Fracture energy, Fractography.

### I. INTRODUCTION

Magnesium material has assumed significant technological importance as structural materials because the newer design and development methodologies, adopting Alumina reinforcements, have resulted in enhancement of the fracture resistance of monolithic Magnesium by several fold [1-6]. Among various Magnesium materials, amorphous Magnesium iniquity combines different to suit several select technological applications [7-10]. These properties include, high melting point combined with high thermal shock resistance and excellent thermal as well as electrical insulating properties [8,10]. However, the mechanical properties of Magnesium material in the monolithic form are far from acceptable levels. Magnesium, in its bulk form, has low strength (both tensile and flexural) and extremely low fracture toughness as compared to several structural ceramic material [8]; thus, needing significant improvements so that it can be accepted for any structural application. One of the means of achieving improved mechanical properties is by using either two- or three dimensional (designated commonly as 2D- and 3D-, respectively) networks of continuous Alumina as reinforcements to the Magnesium -matrix material leading to near structural material, known as Magnesium Metal Matrix Nano Composites. Numerous studies have been conducted in the last two decades on the toughening of this class of Magnesium. These studies have been comprehensively reviewed [2] as well as by [4] and later, by [6]. However, to the best of our knowledge, there are no fracture toughness/energy studies reported so far for the MMNCs,

During the fracture process of a MMMNCs, various event/developments take place in the three regions of the fracture, namely the wake of the crack, at the crack tip and finally in the region of process zone ahead of the crack tip. These influence the net enhancement in the fracture resistance of a MMMNCs. They include some or most of the following [2,3,5].

1. Local increase in the stress level with the application of external loading,
2. Relative displacement of matrix/interface elements,
3. Matrix microcracking, leading to matrix failure (with or without significant crack path meandering, i.e. crack deflection and/or branching),
4. Debonding of matrix interface (with or without significant frictional forces),
5. Frictional sliding of the along the matrix Alumina,
6. Loss of residual strain energy.

These process/stages, schematically in Fig.1, result in significant energy dissipation through frictional events in the wake and process zones, acoustic emission and Magnesium debonding, breakage. Contributions

from these stages of crack tip and fibre reinforcements interactions, with or without the contributions from matrix fracture events, have led to unified models for the fracture resistance in materials that exhibit crack bridging [2-6]. The toughening in these cases of crack bridging is essentially due to ductile or brittle reinforcements. In case of present MMMNCs, it is later that makes contribution to the toughening.

In the present paper, the fracture behaviour of a two-dimensional (2D) Magnesium – Alumina-reinforced, Magnesium - matrix composite is presented and discussed. Various parameters of fracture resistance have been used to quantify the fracture resistance of the material. These include, the plane strain fracture toughness (K<sub>IC</sub>), elastic-plastic fracture toughness (JIC) and total fracture energy release rate (JC). Also reported and discussed are the effects of notch orientation and notch depth on the fracture resistance in these composites.

## II. EXPERIMENTAL PROCEDURE

The composition of nano and micro sized fraction that gives the best mechanical properties, were experimentally determined to be Mg-3.5% vol. Al<sub>2</sub>O<sub>3</sub> [1]. The powders were compacted into a mold of 45x6x3 by cold uniaxial pressing at 30 ton/mm<sup>2</sup>. The compacted samples have been sintered in a Resistance Furnace at the temperature of 630°C for 2 hours in an atmosphere of high purity Argon 15L/Min. In these sintering conditions, established as adequate Oxidation i.e. any loss of Mg was completely prevented. After sintering, the maximum determined weight losses were under 10%.

As compact pressure increases, plastic deformation takes place in the contact zone between the particles starts to break. The porosity in the assembly decreases as particles are squeezed into the remaining free space. The cold welding that occurs during deformation at the inter particle contacts contributes to the strength of the component. Final compactnesses of 78-88%, depending on the compactness after pressing Mg powder. It is more evident in the case of the materials elaborated on the basis of Mg spherical powder. The greater the compacting pressure and the longer the sintering duration the more the compactness reduce.

Single edge notch beam (SENB) specimens of 45x6x3 were used to determine the flexural strength ASTM standard [2] and plane strain. The fracture toughness was evaluated with the help of notches of different initial length introduced in using 0.15 mm thick diamond wafer blade, mounted on a standard Isomet cutting machine. A specially designed jig was used to obtain straight notches by moving the job across the cutting plane. The notches thus introduced were found to have a finite root radius  $\rho$  typically of the order of 100  $\mu$ m. The  $\rho$  values were determined by scanning electron microscope and the crack lengths were found to be in the range of 0.30, 0.45 and 0.60 times the specimen width. Among these, specimens with crack lengths in the range specified by the ASTM standard E-399 (0.45-0.55) times width of specimen were only considered for the determination of K<sub>IC</sub> values. All the fracture toughness tests were conducted on a computer controlled, servo hydraulic Instron 8801 test system using a self-articulating 3-point bend fixture. The tests were conducted at ambient temperature (~25°C) and in laboratory air atmosphere [10,11]. The notched specimens were loaded in ramp control at a constant ramp rate of 0.5 mm/min. Further, K<sub>IQ</sub> values were estimated using the equation

$$K_{IQ} = \frac{P_Q \cdot S}{B \cdot W^{3/2}} f\left(\frac{a}{W}\right) \quad (1)$$

Where,  $f\left(\frac{a}{W}\right) = f(\alpha)$

$$f(\alpha) = 3(\alpha)^{1/2} \cdot (1.99 - \alpha(1-\alpha)(2.15 - 3.93\alpha + 2.7\alpha^2)) / (2(1+2\alpha) \cdot (1-\alpha)^{3/2}) \quad \text{for Bend}$$

where  $P_Q$  = Load (at 5% Seifert offset), B = Thickness, W = Width  
 $S$  = Span of Loading &  $f(a/W)$  = Specimen Geometry Function

P<sub>Q</sub> or P<sub>max</sub> is the load corresponding to the a set of unstable fracture (the determination of values is specified in ASTM Standard E-399 [3], S the span of 3-point bend loading specimen, B the thickness, W the width and a the crack length. The other specimens with larger crack lengths have essentially used to determine the values of total fracture energy release rate (JIC) as per the procedure, dividing in details by Eswara Prasad [4,12]. The load-displacement curves thus obtained were analysed to obtain various measures of fracture resistance, and the results are presented and discussed in the following sections.

Figs.4 (a) show the basic data of the load variation with displacement for the two test specimens obtained from the 3-point bend loading of notched specimen tested of for plane strain fracture toughness, K<sub>IC</sub>. The details of the specimens and the properties derived from these fracture toughness tests have been given in Table 1. The load-displacement curves in Fig.2 clearly indicate that all the specimen fail without noticeable extent of stable curve extension and thus the P<sub>max</sub> values correspond to failure and use of P<sub>max</sub> values in Eq.1 yield K<sub>IC</sub> or K<sub>IQ</sub>. Though specimens with varied a/W ratio were tested, data corresponding to specimens with a/W Values in the range of 0.30-0.60, as specified by ASTM standard E-399, were used to derive K<sub>IC</sub> value. The values of K<sub>max</sub> and K<sub>Q</sub> derived from their tests are also listed in Table 1. The data in Table 1 show that the

material exhibits valid  $K_{max}/KQ$  values ( $<1.1$ ) for all values of  $a/W$  in the range of 0.3-0.6. In view of these observations, the  $KQ$  values derived from specimens with  $a/W$  of 0.30, 0.45 and 0.6 in all case. The values of conditional fracture toughness ( $K_{Ic}$ ) were found to decrease moderately with increase in the crack length. This is due to the change in mode of fracture with increased crack length. At higher crack lengths, the fracture mode gradually changes to predominantly shear, while the same at lower areas lengths ( $a < 0.60 W$ ) is predominantly tensile. This is true for all conditions as is evident from the microstructure.

The values of both  $P_{max}$  (12-25 N) and critical displacement at fracture,  $\delta_{max}$  (0.02-0.04) are also very small, the determination of which requires extremely low capacity low cells and highly sensitive linear variable differential transducers (LVDT). Single edge notch beam (SENB) specimens of 3 mm thickness, 6 mm width and a span length of 45 mm were used. The fracture toughness/energy was evaluated in notch orientations, namely crack divider orientation, in which the notch is along the orientation of the thickness direction.

Notches of varied length were introduced using 0.3 mm thick diamond wafer blades, mounted on a standard Isomet cutting machine. A specially designed jig was used to obtain straight notches by moving the job across the cutting plane. The notches thus introduced were found to have a finite root radius,  $p$ , typically of the order of 160  $\mu m$ . The  $P$  values were determined by Delta TM 35 x-y profile projector. The notch root radii, in the crack divider orientation, were found to be similar. The crack lengths were maintained in the range of 0.30 to 0.6 times the specimen width. Among these, specimens with crack lengths in the range specified by the ASTM standard E-399 [2] (0.45-0.55 times the specimen width) were only considered for the determination of  $K_{Ic}$  values. The other specimens with larger crack lengths were employed essentially to determine the work of fracture [5], which results will be reported separately. The fracture energy determined from the load-displacement data were used to determine the elastic-plastic fracture toughness,  $J_{Ic}$  and the total fracture energy release rate,  $J_c$ . The later two fracture resistance parameters are based on J- integral [6].

All the fracture toughness tests were conducted on a computer controlled, servohydraulic. Instron 8801 rest system using a self-articulating 3-point bend fixtures of MTS 880 test system. The tests were conducted at ambient temperature ( $\sim 230C$ ) and in laboratory air atmosphere. The notched specimens were loaded in ramp control at a constant ramp rate of 0.5 mm/min. The load-displacement curves thus obtained were analysed to obtain various measures of fracture resistance, and the results are presented and discussed in the following sections.

The load-displacement data obtained for crack divider orientations are shown in Figs.3. Crack lengths are given as normalized values (crack length 'a', normalized with the specimen width, 'W'). Though three tests with different  $a/W$  values were conducted in the crack divider direction, for the sake of clarity, only three load – displacement plots are included in Fig. 3. On the other hand, all the three load-displacement plots obtained are included in Fig.3 for the crack divider direction.

### III. FRACTOGRAPHY

SEM fractographs obtained from the specimens tested till failure under flexural (3–point bend loading) testing are shown in Figs.4 Mg-Al<sub>2</sub>O<sub>3</sub> and Al<sub>2</sub>O<sub>3</sub>+ Ni conditions. Though large numbers of fractographs at different magnifications are obtained in each of the two process conditions, for the sake of clarity only one representative fractograph for each condition is included. These fractographs clearly show that Mg material in Mg- Al<sub>2</sub>O<sub>3</sub> and Mg- Al<sub>2</sub>O<sub>3</sub> -Ni conditions fail by mixed fracture comprising of low degree of ductile, microdimples and transgranular shear fracture, with predominant extent of low energy quasi-cleavage faceted fracture[7,8]. In case of Mg- Al<sub>2</sub>O<sub>3</sub>, the size of the quasi-cleavage facets are much finer. This is because of the fact that the Mg material in as Al<sub>2</sub>O<sub>3</sub> condition is of finer grain size as also, because the crystallite size too is much smaller. The fracture facets under these conditions comprise of more cleavage planes where fracture initiated needs to relocate additional facets in the neighbouring grains for further crack extension. Such process needs higher fracture energy as compared to the situation where in the cleavage facets have to encounter less number of grain / crystallite boundaries. In addition, higher the energy required for the fracture process, the material would withstand fracture till higher stresses [8,9]. Such high fracture stresses facilitate the formation of more number of microdimples and higher extent of transgranular shear fracture. Hence, with increasing grain / crystallite size, the facets are much coarser and the extent of microdimples and transgranular shear is much lower (see Fig.4); thus, resulting in much lower flexural strength and fracture energy values  $K_{Ic}$  or  $K_{Ic}$  or  $J_c$  or  $J-R -\Delta a$ . The fact that Mg material with coarser grain resulted in net decrease in the cleavage facet area showing an inverse relation between mechanical property ( $\sigma_f$  or  $K_{Ic}$ ) with the extent of quasi-cleavage fracture facets( %QCF).

The strength and fracture toughness properties of Mg evaluated and reported are the results thus obtained are discussed in terms of the micro structure, grain size and fracture mode in two most widely employed process conditions of as and

S.N	Material Composition	W	B	a	a/W	F(a/W)	P <sub>Q</sub>	P <sub>max</sub>	K <sub>Q</sub>	K <sub>max</sub>	K <sub>ax</sub> /K <sub>Q</sub>	K <sub>IC</sub>
	Magnesium	0.0870	0.0228	0.0261	0.30	1.5212	0.0201	0.0206	0.528	0.5420	1.0265	
A2		0.0841	0.0232	0.0377	0.45	2.2196	0.0264	0.0264	1.0481	0.481	1.000	
A3		0.0846	0.0217	0.0379	0.45	2.2196	0.0185	0.0185	0.7784	0.784	1.000	
A4		0.0866	0.0226	0.0518	0.6	3.6307	0.0325	0.0377	0.2072	0.2475	1.1974	
A5		-	-	-	-	-	-	-	-	-	-	1.04
	Mg+(3.5Al <sub>2</sub> O <sub>3</sub> + 1.5 Ni)	0.0627	0.0206	0.0240	0.30	1.8763	0.0344	0.0344	2.0190	0.190	1.000	
E2		0.0597	0.0235	0.0266	0.47	2.133	0.0164	0.0173	1.0990	0.2542	1.1504	
E3		0.0626	0.0222	0.0281	0.45	2.440	0.02175	0.0223	1.5590	0.441	1.0161	
E4		0.0841	0.0232	0.0377	0.60	3.6410	0.0264	0.0264	1.0081	0.081	1.000	
E5		-	-	-	-	-	-	-	-	-	-	1.56
	Mg+(3.5Al <sub>2</sub> O <sub>3</sub> + 3.0 Ni)	0.0804	0.0239	0.0187	0.23	1.2718	0.0083	0.0091	1.9599	0.337	1.1191	
F2		0.0801	0.0240	0.0249	0.31	1.5608	0.006	0.00619	1.7413	0.7974	1.0322	
F3		0.0799	0.0231	0.0268	0.34	1.6833	0.004266	0.00506	1.9374	0.7994	1.0732	
F4		0.0	0.02	0.0	0.45	2.156	0.0	0.0	2.00	2	1.0	

		671	28	0 2 8 9		5	37 99	39 99	21	. 1 9 5 5	96 5	
F5		-	-	-	-	-	-	-	-	-	-	2.00
D1	Mg+(3.5Al <sub>2</sub> O <sub>3</sub> + 6.0 Ni)	0.0 816	0.02 55	0. 0 2 2 3	0.27	1.409 2	0.1 46 7	0.1 49 5	3.52 06	. 5 8 7 8	1.0 19	
D2		0.0 814	0.02 55	0. 0 3 6 5	0.45	2.310 0	0.0 62	0.0 63 6	2.44 82	. 5 1 1 3	1.0 25	
D3		0.0 699	0.02 06	0. 0 3 5 8	0.51	2.749 1	0.3 80 0	0.0 41	2.86 0	. 0 6 4 4	1.0 79 0	
D4		0.0 84	0.03 0	0. 0 4 8 4	0.58	3.372 7	0.0 38	0.0 47 1	1.77 57	. 2 0 0 9	1.2 39	
D5		-	-	-	-	-	-	-	-	-	-	-

Mg/(3.5Al<sub>2</sub>O<sub>3</sub>),Mg/(3.5Al<sub>2</sub>O<sub>3</sub>+1.5Ni) Mg/(3.5Al<sub>2</sub>O<sub>3</sub>+3.0Ni)and Mg/(3.5Al<sub>2</sub>O<sub>3</sub>+6.0Ni).

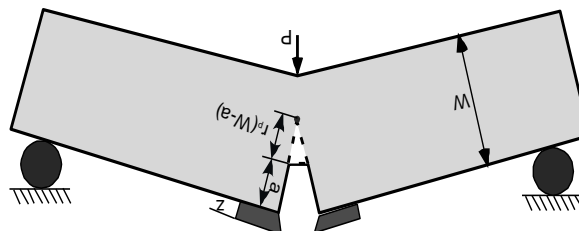


Fig 2 Schematic figure showing the nature of crack extension in b the crack divider orientation.

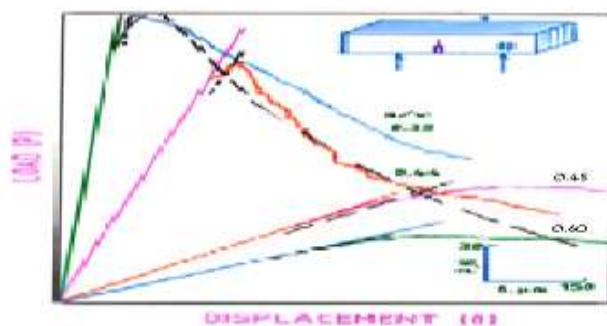


Figure 3: Representative Load-Displacement Curves showing the procedure adopted for the evaluation of total fracture energy release rate ( $J_c$ ) of Mg/(3.5Al<sub>2</sub>O<sub>3</sub>+Ni)

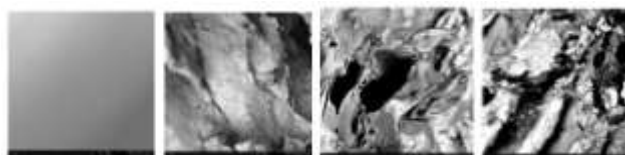


Figure 4: fractographs showing: (a) cleavage failure in pure Mg, (b) localized dimple like structure in Mg/3.5Al<sub>2</sub>O<sub>3</sub>, (c) uniform dimple like features in Mg/(3.5Al<sub>2</sub>O<sub>3</sub>+3.0Ni) and (d) Mg/(3.5Al<sub>2</sub>O<sub>3</sub>+6.0Ni), with predominant crack formations.

#### **IV.CONCLUSIONS**

The MMMNCs material has been comprehensively evaluated for its fracture resistance. These properties pertain to the values at ambient test temperatures. The significant findings are:

1. The MMMNCs material exhibits a grossly different nature of variation in the load with displacement in crack divider arester orientations.
2. The KIC values determined for the material are conservative in nature. The values determined are 2.05 MPa m in the crack divider orientation.
3. The fracture process in the crack divider direction was found to occur under stable conditions, validating all the three fracture toughness parameters evaluated in the present study. The same in the crack arrester direction is less deterministic as the matrix failure occurs under apparent unstable conditions.

#### **REFERENCES**

- [1]. Abel, A. and Ham, R.K.,1966,Acta Metall.,14, 1495.Ashton, R.F., Thompson, D.S., and F.W., 1986, in "Aluminium Alloys – Their physical and Mechanical properties", Vol.I, starke, E.A. and sanders, T.H., eds., Engineering Material Advisory Service, Warley, U.K.,p.403.
- [2]. ASTM Standard E-399,1990, Standard Test Method for plane – Strain Fracture toughness of Mettalic Materials,Annual Book of ASTM standards, Vol.03.01,Section 3, Am.Soc.Testing and Mater., Philadelphia, U.S.A,p.488.
- [3]. ASTM Standard E-561,1990, Standard Practice for R-Curve Determination, Annual book of ASTM Standards, Vol.03.01, Section 3, Am,Soc.Testing and Mater., Philadelphia, U.S.A.,p.571.
- [4]. Eswar Prasad N, Loidal D, Vijayakumar M, Kromp K. Elastic properties of silica-silica continuous fibre-reinforced, ceramic matrix composites.Scripta Mater 2004;50:1121-6.
- [5]. Staley J.T.1976, in "Properties Related to Fracture Toughness", ASTM STP 60s, Am.Soc.Testing and Materials, Metab,Phildelphia, PA, U.S.A., p.71.
- [6]. Shah, R.C., 1974, in "Fracture Analysis",ASTM STP 560, Am.Soc. Testing and Materials, Philadelphia, PA, U.S.A., p.29.
- [7]. Hassan, S.F. and Gupta, M. Development of high strength magnesium: Copper based hybrid composites with enhanced tensile properties Material Science Technology, 19, pp. 253-259. 2003.
- [8]. SF Hassan, M Gupta, Development of ductile magnesium composite materials using titanium as reinforcement, Journals of Alloys Components, 2002, 345, 246-251.
- [9]. N.Eswara Prasad, Sweety Kumari, S.V. Kamat, M. Vijayakumar, and G. Malakondaiah, Fracture behaviour of 2D-weaved, silica-silica continuous fibre-reinforced, ceramic-matrix composites(CFCCs), Engineering Fracture Mechanics 71 (2004) 2589-2605.
- [10]. Townsend, D. and J.E. Field, "Fracture toughness and hardness of zinc sulphide as a function of grain size," Journal of Materials Science, 25,1347-1352 (1990).
- [11]. E.V. Yashina,E.M. Garishchuk, and V.B. IKonnikov, " Mechanisms of Poly crystalline CVD ZnS densification during Hot Isostatic Pressing" Inorganic Material., vol. 40, 9 (2004): pp. 901 - 904.
- [12]. ASTM Standard E-813. Standard test method for J1c ,a measure of fracture toughness. Annual Book of ASTM Standards vol.03.01. West Conshokochen, PA: American Society for Testing and Materials;1997.p.627-41.